

# Solubility and hydrolysis of U(VI) in 0.5 mol/kg NaCl solutions at $T = 22$ and $80\text{ }^{\circ}\text{C}$

Francesco Endrizzi<sup>a,\*</sup>, Xavier Gaona<sup>a,\*</sup>, Maria Marques Fernandes<sup>b</sup>, Bart Baeyens<sup>b</sup>, Marcus Altmaier<sup>a</sup>

<sup>a</sup> Karlsruhe Institute of Technology, Institute for Nuclear Waste Disposal, P.O. Box 3640, 76021 Karlsruhe, Germany

<sup>b</sup> Paul Scherrer Institute, Laboratory for Waste Management, Villigen PSI, CH-5232, Switzerland

## ARTICLE INFO

### Keywords:

Uranium (VI)  
Solubility  
Hydrolysis  
Temperature  
Thermodynamics  
Metaschoepite  
Sodium uranate  
Clarkeite

## ABSTRACT

In this study, the solubility and hydrolysis of U(VI) was investigated at elevated temperature. Experiments were performed in solutions of NaCl 0.51 mol/kg of water in the  $\text{pH}_m$  range 4–13.4 (with  $\text{pH}_m = \log[\text{H}^+]$ ) at  $T = 22 \pm 3$  and  $80 \pm 5\text{ }^{\circ}\text{C}$  under  $\text{N}_2/\text{Ar}$  atmosphere. Two solid phases were used as starting U(VI) materials:  $\text{UO}_3 \cdot 2\text{H}_2\text{O}(\text{cr})$  equilibrated in solutions with  $4 \leq \text{pH}_m \leq 5$  and  $\text{Na}_2\text{U}_2\text{O}_7 \cdot \text{H}_2\text{O}(\text{cr})$  (a synthetic clarkeite like phase) equilibrated in solutions with  $7 \leq \text{pH}_m \leq 13.4$ . The solubility of  $\text{UO}_3 \cdot 2\text{H}_2\text{O}(\text{cr})$  at  $T = 80\text{ }^{\circ}\text{C}$  in the acidic  $\text{pH}_m$  range is decreased by a factor of ten with respect to the U(VI) phase studied at room temperature. Solid phase characterization by XRD, SEM-EDS and quantitative chemical analysis indicate that this decrease is correlated to the transformation of  $\text{UO}_3 \cdot 2\text{H}_2\text{O}(\text{cr})$  into a sodium containing U(VI) solid phase. The solubility of  $\text{Na}_2\text{U}_2\text{O}_7 \cdot \text{H}_2\text{O}(\text{cr})$  in the alkaline  $\text{pH}_m$  range is drastically enhanced at  $T = 80\text{ }^{\circ}\text{C}$ . The main contribution to this effect results from the increased acidity of water at elevated temperature, although an enhanced hydrolytic activity of U(VI) or a decreased stability of  $\text{Na}_2\text{U}_2\text{O}_7 \cdot \text{H}_2\text{O}(\text{cr})$  are also considered, in order to explain the solubility data under these experimental conditions. Solid phase characterization after completing the solubility experiments confirms that  $\text{Na}_2\text{U}_2\text{O}_7 \cdot \text{H}_2\text{O}(\text{cr})$  retains its stoichiometry and structure at  $T = 80\text{ }^{\circ}\text{C}$  within the timeframe of the study ( $t \leq 290$  days). A thermodynamic model, comprising conditional stability constants and enthalpy data has been developed, describing reliably the processes of hydrolytic dissolution of  $\text{Na}_2\text{U}_2\text{O}_7 \cdot \text{H}_2\text{O}(\text{cr})$  in alkaline NaCl solutions up to 0.51 mol/kg and their temperature dependence in the range 22–80  $^{\circ}\text{C}$ .

This work represents the first comprehensive study on U(VI) solubility and hydrolysis at elevated temperatures extending to alkaline  $\text{pH}_m$  conditions relevant in the context of nuclear waste disposal. It provides robust solubility upper limits to be considered in source term estimations, but also thermodynamic data for both solid phases and aqueous species that can be implemented in thermodynamic databases and related geochemical calculations.

## 1. Introduction

Temperature is one of the parameters that will vary during the different operational phases of a high level radioactive waste (HLW) repository. Elevated temperature conditions (up to 200  $^{\circ}\text{C}$ , depending on host rock system and repository concept) will affect the chemistry of radionuclides in the near field of a HLW repository [1,2]. Thus improved knowledge of the solubility and aqueous chemistry of radionuclides at elevated temperature is crucial within the safety assessment of HLW repositories. Thermodynamic data available to date for elevated temperature conditions are

mostly limited to the aqueous equilibria of dissolved radionuclide ions, whereas solubility data for solid phases at temperatures other than ambient conditions are generally rare [3–6].

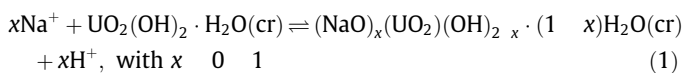
Uranium is a relevant actinide in the context of nuclear waste disposal [7]. Under strongly reducing condition its solubility is expected to be controlled by  $\text{UO}_2(\text{s})$ , whereas under mildly reducing to oxidizing conditions,  $\text{UO}_2(\text{s})$  is not stable and  $(\text{UO}_2)_x(\text{OH})_y^{2x-y}$  species predominate in the aqueous phase [8,9]. In the case of spent nuclear fuel, oxidative dissolution of  $\text{UO}_2(\text{s})$  can be also promoted by oxidants generated by radiolysis of water [2,10]. Depending on the chemical composition of the aquatic system, different U(VI) solid phases will form, such as uranyl hydroxides, carbonates, phosphates or silicates [9]. In particular, the uranyl oxide hydrates schoepite ( $\text{UO}_3 \cdot 2.25\text{H}_2\text{O}(\text{cr})$ ) and metaschoepite ( $\text{UO}_3 \cdot 2\text{H}_2\text{O}(\text{cr})$ ) [9,11–13], sometimes written as the chemically equivalent

\* Corresponding authors.

E-mail addresses: francesco.endrizzi@kit.edu (F. Endrizzi), xavier.gaona@kit.edu (X. Gaona).

UO<sub>2</sub>(OH)<sub>2</sub>·H<sub>2</sub>O(cr)) have been identified as relevant U(VI) solid phases under repository relevant conditions [14,15].

The structure of schoepite and metaschoepite consists of parallel sheets of uranyl pentagonal bipyramids, sharing edges and vertices, while the interlayer regions are occupied by water molecules [16]. Both minerals have a strong tendency to incorporate metal cations in the interlayer regions and to structurally transform [17]. In particular, the incorporation of Na<sup>+</sup>, K<sup>+</sup> and Ca<sup>2+</sup> ions leads to the formation of the stable mineral phases clarkeite (Na(UO<sub>2</sub>)O(OH)<sub>x</sub>H<sub>2</sub>O(cr), with  $x = 0-1$ ), compreignacite (K<sub>2</sub>(UO<sub>2</sub>)<sub>6</sub>O<sub>4</sub>(OH)<sub>6</sub>·8H<sub>2</sub>O(cr)) or becquerelite (Ca(UO<sub>2</sub>)<sub>6</sub>O<sub>4</sub>(OH)<sub>6</sub>·8H<sub>2</sub>O(cr)) [14,17,18]. The gradual transformation of metaschoepite into clarkeite occurs spontaneously over time, according to reaction scheme (1) and is generally favored by high concentrations of dissolved Na<sup>+</sup> and alkaline conditions [14,17,19,20].



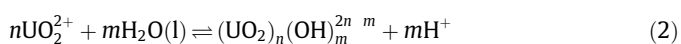
### 1.1. U(VI) hydrolysis and the solubility of U(VI) oxo hydroxides at elevated temperature

A critical, reliable selection of thermodynamic data for U(VI) at  $T = 25^\circ\text{C}$  published until 2003 is provided by the Chemical Thermodynamic Series, Volumes 1 and 5, as part of the NEA Thermochemical Database (NEA TDB project) [9,21]. Values of the hydrolysis constants of the different U(VI) species at temperatures other than  $25^\circ\text{C}$  have also been reported [22], but were not selected in the NEA TDB reviews. More accurate and reliable thermodynamic studies on the hydrolysis of U(VI) at elevated temperatures have been conducted since the publication of the NEA TDB update book in 2003. The most relevant contributions were recently reviewed in different publications [22,23], and are shortly summarized in Section 1.1.1. All thermodynamic quantities reported in the literature for U(VI) hydrolysis species are listed in Table S1 as Supporting Information.

Experimental solubility studies at elevated temperature with U(VI) oxo hydroxides are very scarce [24-27]. Due to significant shortcomings, no thermodynamic data reported in these few studies were selected in the NEA TDB reviews. A short discussion on the information available for these systems is provided in Section 1.1.2.

#### 1.1.1. Hydrolysis of U(VI) at elevated temperature

Thermodynamic studies on the hydrolysis of U(VI) at different temperatures were reported in the literature since the late 1950's [28-30]. Hydrolysis reactions of U(VI), formulated according to the reaction scheme (2), are endothermic processes [3,5,31].



Accordingly, the hydrolysis of uranyl is enhanced by temperature. Despite the rather large number of literature studies, the relative distribution of the different hydrolytic species of U(VI) at temperatures other than  $25^\circ\text{C}$  is still debated and a comprehensive hydrolysis scheme, including the temperature dependence of the hydrolysis constants of U(VI) has not yet been selected in the NEA TDB reviews [9].

In fact, the study of U(VI) hydrolysis in the acidic range is complicated by the known formation of a number of mono- and polynuclear species [9]. According to the NEA TDB selection of U(VI) hydrolysis constants [9], the species UO<sub>2</sub>OH<sup>+</sup> (1,1), (UO<sub>2</sub>)<sub>2</sub>(OH)<sub>2</sub><sup>2+</sup> (2,2), (UO<sub>2</sub>)<sub>3</sub>(OH)<sub>5</sub><sup>3+</sup> (3,5) and (UO<sub>2</sub>)<sub>3</sub>(OH)<sub>7</sub><sup>3,7</sup> (3,7) are predominant in solution at room temperature, under acidic to near neutral pH conditions and a total uranium concentration

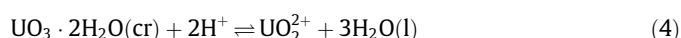
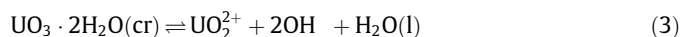
close to the solubility limit of metaschoepite. In the alkaline range ( $\text{pH} > 7$ ) U(VI) forms two monomeric anionic complexes, UO<sub>2</sub>(OH)<sub>3</sub><sup>-</sup> (1,3) and UO<sub>2</sub>(OH)<sub>4</sub><sup>2-</sup> (1,4), the latter one observed in alkaline and hyperalkaline conditions ( $\text{pH} > 11$ ) [9]. Experimental studies in the alkaline range are generally hampered by the low solubility of U(VI) ( $[\text{U}] < 10^{-6}$  mol/kg at room temperature and  $\text{pH} = 7-12$ ), which limits the applicability of several analytical techniques (e.g. potentiometry or spectrophotometry).

After the release of the NEA TDB update book, Zanonato et al. [4] conducted a detailed study of the hydrolysis of UO<sub>2</sub><sup>2+</sup> in the acidic range at variable temperatures (10, 25, 40, 55, 70, 85 °C). (CH<sub>3</sub>CH<sub>2</sub>)<sub>4</sub>NClO<sub>4</sub> 0.10 M was used as background electrolyte. The hydrolysis constants for the species UO<sub>2</sub>OH<sup>+</sup> (1,1), (UO<sub>2</sub>)<sub>2</sub>(OH)<sub>2</sub><sup>2+</sup> (2,2), (UO<sub>2</sub>)<sub>3</sub>(OH)<sub>5</sub><sup>3+</sup> (3,5) were determined by potentiometric titration, using a glass electrode to determine the concentration of H<sup>+</sup> in solution. The corresponding enthalpies were also experimentally determined at each temperature through isothermal microcalorimetry.  $\Delta_r H'_m(1,1)$  was assumed to be temperature independent in the range investigated.  $\Delta_r H'_m(2,2)$  and  $\Delta_r H'_m(3,5)$  showed a linear dependence on temperature and were considered by the authors to calculate  $\Delta_r C_{p,m}(2,2)$  and  $\Delta_r C_{p,m}(3,5)$ .

The same authors extended their work to the study of the hydrolysis of U(VI) in the alkaline range, as part of a broader investigation on the formation of the ternary uranyl hydroxide peroxide complexes in aqueous solution [5,32]. A first study in 2012 was conducted at  $T = 25^\circ\text{C}$ , and focused on potentiometric and spectrophotometric titrations [32]. In a second study published in 2014 [5], Zanonato and co workers used isothermal microcalorimetry to determine enthalpy data for the U(VI) hydrolysis species identified. Both studies used [(CH<sub>3</sub>)<sub>4</sub>N]NO<sub>3</sub> (TMA NO<sub>3</sub>) as background electrolyte to minimize the precipitation of U(VI) under alkaline pH conditions. The chemical model proposed for the alkaline pH range included the hydrolysis species UO<sub>2</sub>(OH)<sub>3</sub><sup>-</sup> (1,3), UO<sub>2</sub>(OH)<sub>4</sub><sup>2-</sup> (1,4) and (UO<sub>2</sub>)<sub>3</sub>(OH)<sub>8</sub><sup>3,8</sup> (3,8). For UO<sub>2</sub>(OH)<sub>3</sub><sup>-</sup> the authors calculated  $\log^* \beta'_{(1,3)} = (18.81 \pm 0.17)$  in 0.1 TMA NO<sub>3</sub>. This value is noticeably different with respect to the one selected by the NEA TDB at  $I = 0$ ,  $\log^* \beta^0_{(1,3)} = (20.25 \pm 0.42)$  [9]. This difference is likely related to the high U(VI) concentrations used by Zanonato and co workers (expectedly promoting the predominance of polyatomic species) and the poorly defined interaction of the bulky cation TMA<sup>+</sup> with the anionic species UO<sub>2</sub>(OH)<sub>3</sub><sup>-</sup>. The use of thermodynamic data determined in such highly artificial background electrolyte for calculations on aqueous systems containing the main inorganic salts (e.g. NaCl, KCl, CaCl<sub>2</sub>, MgCl<sub>2</sub>, NaNO<sub>3</sub>) relevant in repository sites appears questionable.

#### 1.1.2. Solubility of UO<sub>3</sub>·2H<sub>2</sub>O(cr) and Na<sub>2</sub>U<sub>2</sub>O<sub>7</sub>·H<sub>2</sub>O(cr) at elevated temperatures

The value of the standard solubility product selected by NEA TDB for crystalline metaschoepite, UO<sub>3</sub>·2H<sub>2</sub>O(cr), (3) is  $\log K^{\circ}_{s,0} = (23.19 \pm 0.43)$  [9,21]. For the hydrolytic dissolution of UO<sub>3</sub>·2H<sub>2</sub>O(cr) (4) a value of  $\log^* K^{\circ}_{s,0} = (4.81 \pm 0.43)$  is obtained using  $\log K^{\circ}_w = 14.00$ . The value of  $\log K^{\circ}_{s,0}$  is calculated internally from enthalpy and entropy data determined in calorimetric studies [33-35]. The latter studies were performed with a highly crystalline UO<sub>3</sub>·2H<sub>2</sub>O(cr) material, obtained by the hydration of anhydrous UO<sub>3</sub>(cr) synthesized at  $T = 500-600^\circ\text{C}$ . Note that our recent solubility study conducted with a crystalline UO<sub>3</sub>·2H<sub>2</sub>O(cr) precipitated at room temperature resulted in a slightly higher solubility constant,  $\log^* K^{\circ}_{s,0} = (5.35 \pm 0.13)$  [20].



The current NEA TDB selection of reaction enthalpy for the hydrolytic dissolution of metaschoepite [21] does not comprise

any thermodynamic data obtained in solubility studies at elevated temperatures [26,27,29,30,36,37]. Relevant shortcomings in these publications were identified by the NEA TDB review team, especially regarding the absent (or limited) information on the solid phase characterization after completing the solubility experiments at elevated temperatures. The reader is referred to Grenthe et al. [21] and Guillaumont et al. [9] for a detailed discussion of these studies. Experimental data and thermodynamic quantities reported in the original publications are summarized in Fig. S 1 and Table S 1 as Supporting Information.

The solubility study by Nikolaeva and Pirozhkov [25] was not reviewed in Grenthe et al. [21] and is therefore shortly summarized here. The authors investigated the solubility of  $\text{UO}_3 \cdot 2\text{H}_2\text{O}(\text{cr})$  at  $T = 22 - 150^\circ\text{C}$ . The pH of the solubility samples was adjusted to 3.5 - 4.9 with either  $\text{HClO}_4$  or  $\text{HNO}_3$ . No additional background electrolyte to maintain constant ionic strength was present in solution. No solid phase characterization was performed after completing the solubility experiments at elevated temperature, and thus the assumption of the solid phase controlling the solubility in these conditions remains speculative. Original data reported by the authors are summarized in Fig. S1 and Table S6 as Supporting Information.

Literature data on the solubility of sodium uranate solid phases are very scarce and limited to systems at  $25^\circ\text{C}$  [14,17,38,39]. A detailed discussion on the available solubility data at room temperature is provided in Altmaier et al. [20]. The present study is, to the best of our knowledge, the first attempt to quantitatively assess the impact of temperature on the solubility of U(VI) at alkaline to hyperalkaline  $\text{pH}_m$  conditions. Solid phases were thoroughly characterized before and after completing the solubility experiments, with the aim of evaluating the stability of the starting solid phases and identify possible solid phase transformations occurring at elevated temperatures.

## 2. Experimental

### 2.1. Chemicals

$\text{NaOH}$  Titrisol<sup>®</sup>,  $\text{HCl}$  Titrisol<sup>®</sup> solutions ( $1.00 \text{ mol dm}^{-3}$ , standardized by the manufacturer), and Suprapur<sup>®</sup> grade  $\text{HNO}_3$  (65%) were purchased from Merck and used without any further purification. All solutions were prepared using Milli Q deionized water ( $18.2 \text{ M}\Omega$ , Merck Millipore) and handled in  $\text{N}_2/\text{Ar}$  gloveboxes to exclude  $\text{CO}_2$ .

Stock solutions of  $\text{NaOH}$  and  $\text{HCl}$  ( $0.5 \text{ mol dm}^{-3}$ ) were prepared at  $T = 22^\circ\text{C}$  and standardized against the primary standards  $\text{KH}(\text{phtalate})$  (pur. > 99.99%, Aldrich) and  $\text{NH}_2\text{C}(\text{CH}_2\text{OH})_3$  (pur. > 99.99%, Aldrich), respectively, according to published procedures, using a glass electrode to determine the equivalent point [40]. The concentration of the two stocks was determined within  $\pm 0.002 \text{ mol dm}^{-3}$ .

$\text{NaCl}$  (p.a., Merck) was preliminarily dried at  $150^\circ\text{C}$ . A stock solution of  $\text{NaCl}$   $0.500 \pm 0.01 \text{ mol dm}^{-3}$  was prepared at  $T = 22^\circ\text{C}$  by weight.

Concentrations of the different stock solutions, obtained in the molar units ( $\text{mol dm}^{-3}$ ) were then converted to  $\text{mol/kg}$  of water ( $\text{mol/kg}$ ) using the conversion factors reported by NEA TDB for different background electrolytes [9].

Metaschoepite ( $\text{UO}_3 \cdot 2\text{H}_2\text{O}(\text{cr})$ ) and sodium uranate ( $\text{Na}_2\text{U}_2\text{O}_7 \cdot \text{H}_2\text{O}(\text{cr})$ ) solid phases synthesized in a previous solubility study by KIT INE at room temperature were used in the present work [20]. X ray diffraction (XRD) patterns of the dried powders were consistent with those of crystalline metaschoepite (JCPDS file 43 0364) and with those of a clarkeite like solid (JCPDS file 50 1586). A further characterization of these solid phases by

quantitative chemical analyses, differential thermal analysis (DTA) and scanning electron microscopy with X ray analysis of the scattered electrons (SEM EDS) was consistent with the elemental composition of the indicated compounds (see section 2.3). SEM analysis revealed the expected platelet like structure of the crystals with an average diameter of  $0.5 - 3 \mu\text{m}$ .

Note that the chemical formula of the sodium uranate solid phase used in the present study and in Altmaier et al. [20] can be equally defined as  $\text{Na}_2\text{U}_2\text{O}_7 \cdot \text{H}_2\text{O}(\text{cr})$  or  $\text{NaUO}_2\text{O}(\text{OH})(\text{cr})$ . The former has been preferred throughout this work.

### 2.2. $\text{pH}_m$ measurements

The  $\text{H}^+$  concentration was measured with a combination glass electrode (Orion ROSS). In samples with a known high initial concentration of  $[\text{OH}^-]$  which can be assumed to be stable throughout the studies ( $[\text{OH}^-] > 0.03 \text{ m}$ ),  $\text{pH}_m$  was calculated from known  $[\text{OH}^-]$  and the conditional  $K_w'$ . Samples were not strictly thermostated during the pH measurements at elevated temperature. Typically, the maximum temperature decrease in solution before equilibration of the electrode did not exceed  $5^\circ\text{C}$ . Prior to the sampling, the electrode was calibrated against diluted commercial pH buffer solutions at  $T = 22$  or  $80^\circ\text{C}$  (Merck, pH 2 - 12 at  $T = 20^\circ\text{C}$ , the corresponding pH values at  $T = 80^\circ\text{C}$  were provided by the manufacturer) to relate the potential of the electrode to a value of  $\text{pH}_{\text{exp}}$  according to the Nernst's law. The value of  $\text{pH}_m$  ( $-\log[\text{H}^+]$ ) was calculated as  $\text{pH}_m = \text{pH}_{\text{exp}} + A_m$ , where  $A_m$  is an empirical parameter accounting for both the junction potential of the electrode and the activity of  $\text{H}^+$ .  $A_m$  is a function of the ionic medium and temperature. Values required for pH measurements at  $T = 22^\circ\text{C}$  were taken from the literature [20], whereas  $A_m$  values at  $T = 80^\circ\text{C}$  were experimentally determined in the present study by measuring the electrodic potential of  $\text{HCl}$  solutions with defined concentrations (from  $1.25 \cdot 10^{-3}$  to  $0.02 \text{ m}$ ) prepared in  $0.51 \text{ mol/kg}$   $\text{NaCl}$   $\text{HCl}$  at  $T = 80^\circ\text{C}$ .

### 2.3. Solubility experiments

Batch solubility experiments from undersaturation conditions were performed in  $0.51 \text{ mol/kg}$   $\text{NaCl}$  at  $T = (80 \pm 5)^\circ\text{C}$ . Standardized  $\text{HCl}/\text{NaOH}/\text{NaCl}$  stock solutions were used to adjust  $\text{pH}_m$  at constant ionic strength. Solutions in the  $\text{pH}_m$  range 4 to 5 were equilibrated with  $\text{UO}_3 \cdot 2\text{H}_2\text{O}(\text{cr})$ , while solutions in the  $\text{pH}_m$  range 7 to 12 were equilibrated with  $\text{Na}_2\text{U}_2\text{O}_7 \cdot \text{H}_2\text{O}(\text{cr})$ . Batches consisting of  $5 - 10 \text{ mg}$  of solid phase contacted with  $20 \text{ mL}$  of supernatant were prepared in screw cap PTFE vials (Semadeni Plastic Group, Switzerland) and stored in an oven placed in the glovebox. To ensure that the PTFE vials are chemically inert at  $T = 80^\circ\text{C}$  (i.e. no release of organic compounds), test vials were filled with  $0.51 \text{ mol/kg}$   $\text{NaCl}$   $\text{HCl}$  or  $\text{NaCl}$   $\text{NaOH}$  solutions at  $\text{pH}_m = 4 - 13.7$ , equilibrated for 30 days at  $T = 80^\circ\text{C}$ . Total organic carbon analysis (TOC, measured with Shimadzu TOC5000) indicated no organic contribution above trace level concentration ( $\sim 0.1 \text{ ppm}$  detection limit).  $\text{pH}_m$  and  $[\text{U}]$  were measured at regular time intervals from 5 to 290 days. U concentration was determined by Inductively Coupled Plasma Mass Spectrometry (ICP MS, Perkin Elmer ELAN 6100) after separation of the solid phase and dilution of an aliquot ( $0.100 \text{ mL}$ ) of the supernatant into 2%  $\text{HNO}_3$  aqueous solution. A further dilution was usually needed, to obtain a total uranium concentration in the sample of about  $1.0 - 10 \text{ mg/kg}$ , the optimal concentration range for the ICP MS instrument used. In addition, a maximum concentration of  $\text{NaCl} \sim 50 \text{ mg/kg}$  was allowed, above which the instrument could not be reliably operated. Three different approaches were used for phase separation: (i) rapid syringe filtration (Pall Acrodisc<sup>®</sup> filters, pore size  $0.1 \mu\text{m}$ , PTFE membrane). This step was performed within  $t < 10 \text{ s}$  and involved a slight



decrease in temperature of the filtrate to  $T > 70$  °C; (ii) ultrafiltration with 10 kD filters (NanoSep Merck Millipore, pore size  $\approx 2$  nm). This separation method required  $t \approx 5$  min, leading to the decrease of the temperature to almost ambient conditions; (iii) direct pipetting of the decanted supernatant with no decrease in temperature. The comparison of [U] after these steps indicated no impact of the separation method on the measured U concentration. Five or more samplings of the same batch were performed overtime after the equilibrium was reached. This ensured, besides the attainment of the equilibration conditions, the reproducibility of the measured concentrations and a sufficiently high population of statistical data to be modeled.

At the end of the solubility study at  $T = 80$  °C, the solid phases were separated from the supernatant, washed with milliQ water, dried under  $N_2$  atmosphere and characterized using XRD, SEM EDS and quantitative chemical analysis. XRD measurements were performed with a Bruker AXS D8 Advance X ray powder diffractometer at  $5 \leq 2\theta \leq 60^\circ$  with incremental steps of  $0.01^\circ$  to  $0.04^\circ$  and a measurement time of 4 30 s per step. Characterization of the solid phases by SEM EDS was conducted with a CamScan FE44 SEM equipped with a Noran EDS unit. The elemental composition of the solid phases (Na, U) was determined by means of Inductively Coupled Plasma Optical Emission Spectroscopy (ICP OES). After repeatedly washing the solid phase with ethanol to remove adherent matrix solution and dissolving the solid into 2%  $HNO_3$ , the samples were diluted to  $[U] \sim 10$ –80 ppm and both [U] and [Na] measured.

The solid phases of  $Na_2U_2O_7 \cdot H_2O(cr)$  collected after finalizing the solubility experiments at elevated temperature were used to conduct a second solubility study at  $T = (22 \pm 3)$  °C. This aimed at assessing the impact of solid phase tempering at  $T = 80$  °C on the solubility of  $Na_2U_2O_7 \cdot H_2O(cr)$  determined at ambient temperature conditions. Batch solubility samples were prepared in 0.51 mol/kg NaCl NaOH solutions with  $8 \leq pH_m \leq 13.5$  following the same approach as described above, with phase separation only conducted by 10 kD ultrafiltration. Solubility data obtained at  $T = 22$  °C are compared to our solubility study using a non tempered  $Na_2U_2O_7 \cdot H_2O(cr)$  solid phase [20].

#### 2.4. Thermodynamic model

The present work extends a previous study by Altmaier et al. [20]. The authors performed a comprehensive study on the solubility of  $UO_3 \cdot 2H_2O(cr)$  and  $Na_2U_2O_7 \cdot H_2O(cr)$  at  $T = (22 \pm 2)$  °C in dilute to concentrated NaCl solutions (0.03–5.61 mol/kg NaCl). The work presents a consistent chemical and thermodynamic model including the solubility products of the two solid U(VI) phases, hydrolysis constants of U(VI) hydrolysis species relevant over the acidic to alkaline range, and values for ion interaction parameters according to the Specific Ion Interaction Theory (SIT) [41]. In this model, the values of the hydrolysis constants of U(VI) in the acidic range (Supporting Information, Table S2) are taken from NEA TDB [9], whereas new values of the hydrolysis constants were determined for the species  $UO_2(OH)_3$  and  $UO_2(OH)_4^{2-}$  predominating in the alkaline range (Supporting Information, Table S2) [20]. The same speciation scheme has been considered in the present work for the interpretation and modelling of the current solubility data at room temperature.

### 3. Results and discussion

#### 3.1. Solubility of $UO_3 \cdot 2H_2O(cr)$ and $Na_2U_2O_7 \cdot H_2O(cr)$

The solubility data of  $UO_3 \cdot 2H_2O(cr)$  and  $Na_2U_2O_7 \cdot H_2O(cr)$  determined at  $T = 80$  °C are shown in Fig. 1 as red symbols. Analytical

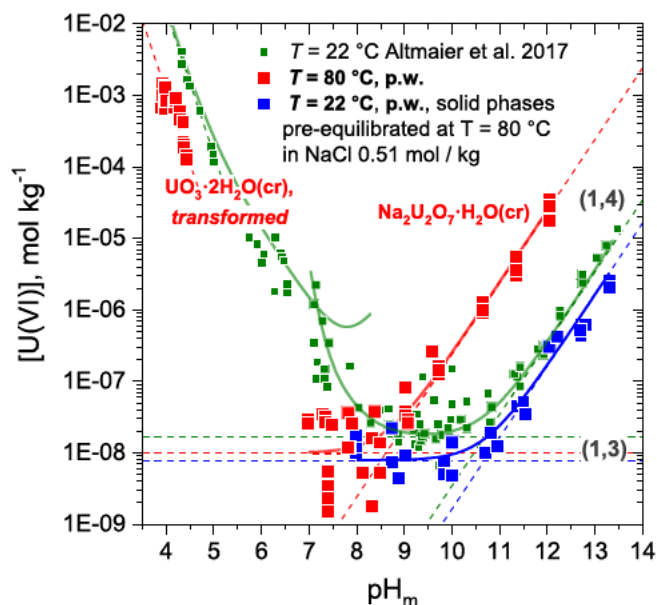


Fig. 1. Solubility of  $UO_3 \cdot 2H_2O(cr)$  and  $Na_2U_2O_7 \cdot H_2O(cr)$  in 0.51 mol/kg NaCl solutions. Red symbols: experimental data at  $T = 80$  °C (p.w.); blue symbols: experimental data at  $T = 22$  °C with  $Na_2U_2O_7 \cdot H_2O(cr)$  tempered at  $T = 80$  °C (p.w.); green symbols: experimental data at  $T = 22$  °C with non-tempered  $Na_2U_2O_7 \cdot H_2O(cr)$  (Altmaier et al. [20]). Solid green line corresponds to the solubility of  $UO_3 \cdot 2H_2O(cr)$  and  $Na_2U_2O_7 \cdot H_2O(cr)$  in 0.51 mol/kg NaCl solutions calculated using thermodynamic and SIT activity models derived in Altmaier et al. [20]. Solid blue and red lines correspond to the solubility of  $Na_2U_2O_7 \cdot H_2O(cr)$  in 0.51 mol/kg NaCl solutions at  $T = 22$  and  $80$  °C, respectively, calculated with the thermodynamic model derived in the present work. Concentrations are reported as mol/kg of water. (For interpretation of the references to colour in this figure legend, the reader is referred to the web version of this article.)

data are tabulated in Table S4 in the supporting materials. The figure also shows the solubility data at  $T = 22$  °C obtained in the present study using a  $Na_2U_2O_7 \cdot H_2O(cr)$  solid previously equilibrated at  $T = 80$  °C in 0.51 mol/kg NaCl solutions (blue symbols). Green symbols in Fig. 1 correspond to the solubility data at  $T = 22$  °C reported by Altmaier et al. [20] for  $UO_3 \cdot 2H_2O(cr)$  and  $Na_2U_2O_7 \cdot H_2O(cr)$  solid phases precipitated and studied at room temperature.

In the acidic region, the solubility of  $UO_3 \cdot 2H_2O(cr)$  at  $T = 80$  °C is  $\approx 1$  order of magnitude lower than the corresponding solubility of the same phase measured at  $T = 22$  °C [20]. The solubility curves as function of  $pH_m$  follow a similar nearly linear trend with a slope ( $\log[U]$  vs  $pH_m$ ) of  $\sim 2$  at both temperatures, indicating that solubility is controlled by equilibrium processes consuming two  $H^+$ .

The solubility data in acidic NaCl solutions at  $T = 80$  °C compare well with the solubility study conducted by Nikolaeva and Pirozhkov with  $UO_3 \cdot 2H_2O(cr)$  at  $T = 70$  and  $90$  °C [25] (see Fig. S1 as Supporting Information). Data reported by the latter authors at  $T = 22$  °C are also in moderate agreement with observations reported by Altmaier et al. [20] under analogous pH and temperature conditions.

In the near neutral to moderately alkaline  $pH_m$  range (8–10 at  $T = 22$  °C, 7.5–8.5 at  $T = 80$  °C) the solubility of  $Na_2U_2O_7 \cdot H_2O(cr)$  is not significantly affected by temperature. In this  $pH_m$  region, the measured U(VI) concentrations at  $T = 80$  °C and  $T = 22$  °C (referring to a tempered  $Na_2U_2O_7 \cdot H_2O(cr)$  solid phase) are similar ( $0.3$ – $3$ )  $\cdot 10^{-8}$  mol/kg and in line with previous results obtained at  $T = 22$  °C with a non tempered Na uranate solid phase [20]. The concentration of uranium in this  $pH_m$  region is near the detection limit of the analytical technique used for the quantification. A relatively high uncertainty (on average  $\pm 0.4$  orders of magnitude) is associated with each measurement. At both investigated temperatures, the solubility of  $Na_2U_2O_7 \cdot H_2O(cr)$  is mostly independent of



$\text{pH}_m$ , indicating that no  $\text{H}^+$  are involved in the solution equilibria controlling the solubility of U(VI) in this  $\text{pH}_m$  region.

In the alkaline and hyperalkaline  $\text{pH}_m$  range ( $\text{pH}_m$  above  $\approx 10$ ), the solubility of  $\text{Na}_2\text{U}_2\text{O}_7 \cdot \text{H}_2\text{O}(\text{cr})$  is enhanced by about 2 orders of magnitude at  $T = 80^\circ\text{C}$  compared to the corresponding solubility of Na Uranate at  $T = 22^\circ\text{C}$ . At room temperature, the solubility of the tempered  $\text{Na}_2\text{U}_2\text{O}_7 \cdot \text{H}_2\text{O}(\text{cr})$  previously equilibrated at  $T = 80^\circ\text{C}$  is slightly decreased compared to the non tempered phase, indicating only a minor impact of temperature on the crystallinity of the solid phase. In all cases, the solubility in this  $\text{pH}_m$  region follows a well defined slope of +1 ( $\log[\text{U}]$  vs  $\text{pH}_m$ ), indicating the formation of anionic hydrolysis species accompanied by the release of one  $\text{H}^+$  in solution.

### 3.2. Solid phase characterization

The U(VI) solid phases investigated in this study were characterized before and after the solubility experiments at  $T = 80^\circ\text{C}$ . Fig. 2 shows the XRD diffraction patterns of the initial  $\text{UO}_3 \cdot 2\text{H}_2\text{O}(\text{cr})$  (a) and  $\text{Na}_2\text{U}_2\text{O}_7 \cdot \text{H}_2\text{O}(\text{cr})$  (c) solid phases. The XRD patterns of selected solid phases isolated at the end of the solubility experiments at  $T = 80^\circ\text{C}$  are also shown (b, d, e). The XRD references available in the JCPDS crystallographic database for  $\text{UO}_3 \cdot 2\text{H}_2\text{O}(\text{cr})$  (JCPDS File 43 0364 [42]),  $\text{Na}(\text{UO}_2)\text{O}(\text{OH}) \cdot x\text{H}_2\text{O}(\text{cr})$  (clarkeite, JCPDS File 50 1586 [43]) and  $\text{Na}_2\text{U}_3\text{O}_{10} \cdot \text{H}_2\text{O}(\text{cr})$  (JCPDS File 41 0840 [44]) are displayed in the same figure for comparison.

The initial solid phases  $\text{UO}_3 \cdot 2\text{H}_2\text{O}(\text{cr})$  (Fig. 2a) and  $\text{Na}_2\text{U}_2\text{O}_7 \cdot \text{H}_2\text{O}(\text{cr})$  (Fig. 2c) were characterized as microcrystalline materials, featuring XRD patterns consistent with the one of the reference material (bottom diagram, relevant peaks:  $\text{UO}_3 \cdot 2\text{H}_2\text{O}(\text{cr})$ ,  $2\theta = 12.1^\circ, 24.3^\circ, 24.8^\circ, 25.5^\circ, 28.3^\circ, 35.0^\circ, 35.5^\circ$ ;  $\text{Na}(\text{UO}_2)\text{O}(\text{OH})$  (cr),  $2\theta = 15.0^\circ, 26.5^\circ, 30.3^\circ, 45.9^\circ, 48.5^\circ$ ). XRD patterns collected for  $\text{UO}_3 \cdot 2\text{H}_2\text{O}(\text{cr})$  after completing the solubility experiments at  $T = 80^\circ\text{C}$  in 0.51 mol/kg NaCl solution at  $\text{pH}_m = 4.2$  are shown in Fig. 2b. These patterns differ significantly from those of the initial material (Fig. 2a), indicating a solid phase transformation during the solubility experiments at  $T = 80^\circ\text{C}$ . The intense peak at  $2\theta = 12.1^\circ$  characteristic of  $\text{UO}_3 \cdot 2\text{H}_2\text{O}(\text{cr})$  disappears, while two sharp peaks at  $2\theta = 15.0^\circ, 26.5^\circ$  observed for the tempered phases resemble those of  $\text{Na}_2\text{U}_2\text{O}_7 \cdot \text{H}_2\text{O}(\text{cr})$  or  $\text{Na}_2\text{U}_3\text{O}_{10} \cdot \text{H}_2\text{O}(\text{cr})$ , pointing towards the formation of a sodium uranate like phase.

XRD patterns of  $\text{Na}_2\text{U}_2\text{O}_7 \cdot \text{H}_2\text{O}(\text{cr})$  collected after solubility experiments at  $T = 80^\circ\text{C}$  (Fig. 2d and e) indicate no relevant impact of the temperature on the solid phase morphology and crystallinity, regardless of the  $\text{pH}_m$  conditions during the equilibration ( $\text{pH}_m = 8.5$  in Fig. 2d;  $\text{pH}_m = 11.5$  in Fig. 2e). The slightly lower solubility at room temperature of  $\text{Na}_2\text{U}_2\text{O}_7 \cdot \text{H}_2\text{O}(\text{cr})$  previously equilibrated at  $T = 80^\circ\text{C}$  (see Fig. 1, blue symbols), with respect to the non tempered  $\text{Na}_2\text{U}_2\text{O}_7 \cdot \text{H}_2\text{O}(\text{cr})$  (green symbols in Fig. 1, Altmaier et al. [20]) cannot be directly linked to the XRD results where large changes in crystallinity are evidenced by changes in peak width. The difference between the two solubility series is nonetheless small, especially considering the relatively high dispersion of the data points in the  $\text{pH}_m$  range 7–11.

Fig. 3 shows SEM images of U(VI) solid phases collected before and after performing the solubility experiments at  $T = 80^\circ\text{C}$ . The two initial solid phases  $\text{UO}_3 \cdot 2\text{H}_2\text{O}(\text{cr})$  (Fig. 3a) and  $\text{Na}_2\text{U}_2\text{O}_7 \cdot \text{H}_2\text{O}(\text{cr})$  (Fig. 3b) show the typical platelet like morphology [17] and a diameter of about  $1.2 \mu\text{m}$  ( $\text{UO}_3 \cdot 2\text{H}_2\text{O}(\text{cr})$ ) and  $0.5 \sim 1 \mu\text{m}$  ( $\text{Na}_2\text{U}_2\text{O}_7 \cdot \text{H}_2\text{O}(\text{cr})$ ) [12]. A SEM image of the transformed  $\text{UO}_3 \cdot 2\text{H}_2\text{O}(\text{cr})$  equilibrated at  $T = 80^\circ\text{C}$  in 0.51 mol/kg NaCl at  $\text{pH}_m = 4.2$  is shown in Fig. 3c. Morphologically, the crystallites of this solid appear smaller than those in the original material (Fig. 3a), with an average diameter  $< 1 \mu\text{m}$ , more similar to  $\text{Na}_2\text{U}_2\text{O}_7 \cdot \text{H}_2\text{O}(\text{cr})$  (Fig. 3b). Elemental analyses of selected solid phases using EDS scattering are summarized in

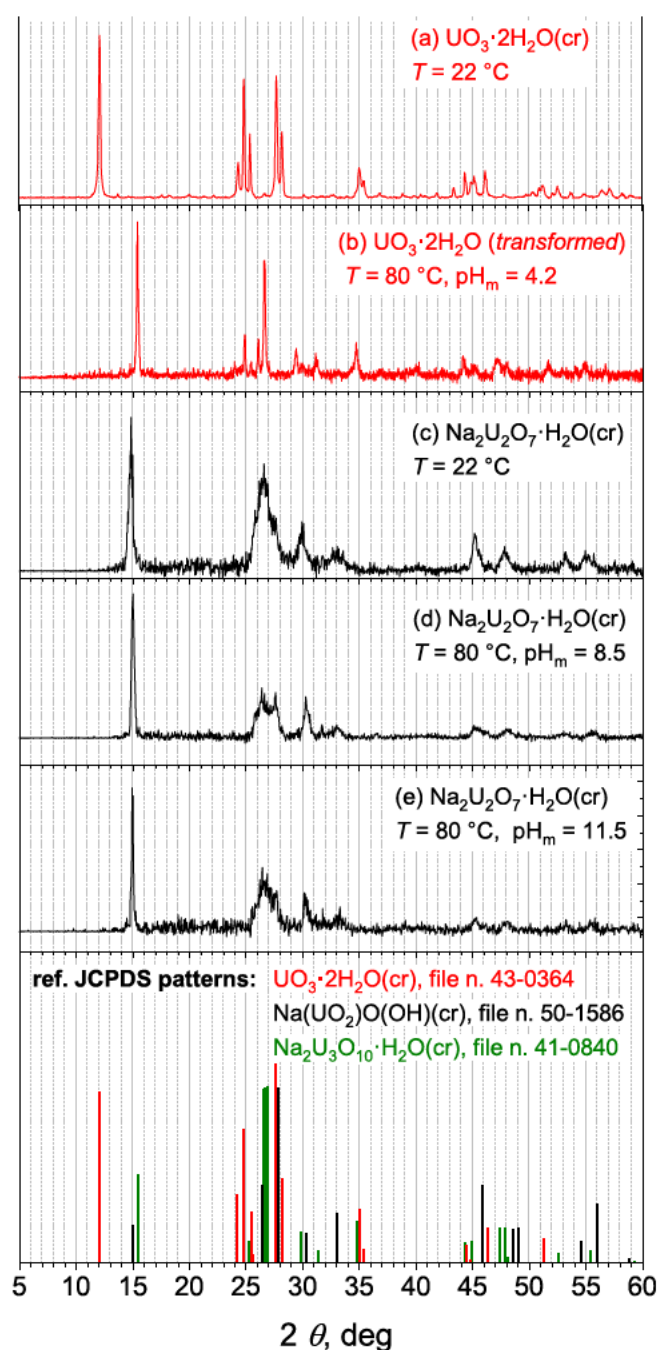


Fig. 2. Powder XRD patterns of U(VI) solid phases investigated in this study: (a)  $\text{UO}_3 \cdot 2\text{H}_2\text{O}(\text{cr})$  before experiments at  $T = 80^\circ\text{C}$ . (b) transformed  $\text{UO}_3 \cdot 2\text{H}_2\text{O}(\text{cr})$  equilibrated for 290 days at  $T = 80^\circ\text{C}$  in a 0.51 mol/kg NaCl solution with  $\text{pH}_m = 4.2$ . (c)  $\text{Na}_2\text{U}_2\text{O}_7 \cdot \text{H}_2\text{O}(\text{cr})$  before experiments at  $T = 80^\circ\text{C}$ . (d)  $\text{Na}_2\text{U}_2\text{O}_7 \cdot \text{H}_2\text{O}(\text{cr})$  equilibrated for 290 d at  $T = 80^\circ\text{C}$  in 0.51 mol/kg NaCl solutions at  $\text{pH}_m = 8.5$  and 11.5 (e). (f) Reference patterns for  $\text{Na}(\text{UO}_2)\text{O}(\text{OH})$ (cr) (black lines, JCPDS file 50-1586 [43]),  $\text{UO}_3 \cdot 2\text{H}_2\text{O}(\text{cr})$  (red lines, JCPDS file 43-0364[42]) and  $\text{Na}_2\text{U}_3\text{O}_{10} \cdot \text{H}_2\text{O}(\text{cr})$  (green lines, JCPDS file 41-0840 [44]). (For interpretation of the references to colour in this figure legend, the reader is referred to the web version of this article.)

Table 1. Temperature has no impact on the ratio Na:U in  $\text{Na}_2\text{U}_2\text{O}_7 \cdot \text{H}_2\text{O}(\text{cr})$ . On the contrary, EDS analysis revealed the presence of sodium with an average molar ratio  $\text{Na}:\text{U} = (0.3 \pm 0.2)$  in the transformed  $\text{UO}_3 \cdot 2\text{H}_2\text{O}(\text{cr})$  equilibrated at  $T = 80^\circ\text{C}$ . Chlorine was not detected, indicating that the transformed phase does not incorporate Cl in its structure. Both EDS and XRD also exclude the presence of NaCl in any of the investigated solids.

Table 1 also summarizes the ratio Na:U in selected solid phases as determined by quantitative chemical analysis. A ratio of  $\approx 1$  is

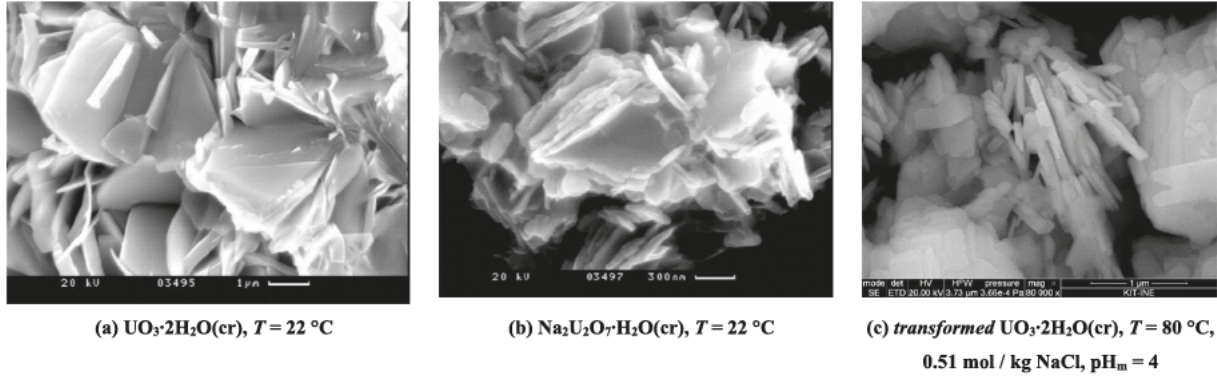


Fig. 3. SEM images of: (a)  $\text{UO}_3 \cdot 2\text{H}_2\text{O}(\text{cr})$  original material synthesized at  $T = 22\text{ }^\circ\text{C}$ ; (b)  $\text{Na}_2\text{U}_2\text{O}_7 \cdot \text{H}_2\text{O}(\text{cr})$  original material synthesized at  $T = 22\text{ }^\circ\text{C}$ ; (c) transformed  $\text{UO}_3 \cdot 2\text{H}_2\text{O}(\text{cr})$  equilibrated at  $T = 80\text{ }^\circ\text{C}$  in a 0.51 mol/kg NaCl solution at  $\text{pH}_m = 4.2$ .

Table 1

Na:U ratio in the investigated U(VI) solid phases, determined by SEM-EDS and quantitative chemical analysis. Relative uncertainties are reported as 1 standard deviation, accounting for 68% confidence interval.

Solid phase	Na:U (SEM-EDS)	Na:U (chemical analysis)
$\text{UO}_3 \cdot 2\text{H}_2\text{O}(\text{cr})$ original material	no Na detected	n. m.
Transformed $\text{UO}_3 \cdot 2\text{H}_2\text{O}(\text{cr})$ after equilibration $T = 80\text{ }^\circ\text{C}$	$(0.3 \pm 0.2)$	$(0.4 \pm 0.1)$
$\text{Na}_2\text{U}_2\text{O}_7 \cdot \text{H}_2\text{O}(\text{cr})$ original material	n. m.	$(0.9 \pm 0.1)$
$\text{Na}_2\text{U}_2\text{O}_7 \cdot \text{H}_2\text{O}(\text{cr})$ after equilibration $T = 80\text{ }^\circ\text{C}$	$(1.0 \pm 0.1)$	$(1.0 \pm 0.1)$

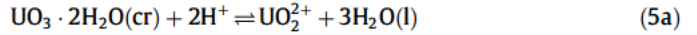
n.m.: not measured.

quantified for  $\text{Na}_2\text{U}_2\text{O}_7 \cdot \text{H}_2\text{O}(\text{cr})$  solid phases before and after tempering at  $T = 80\text{ }^\circ\text{C}$ , consistent with XRD and SEM EDS observations. ICP OES results also indicated a Na:U ratio of  $(0.4 \pm 0.1)$  in the  $\text{UO}_3 \cdot 2\text{H}_2\text{O}(\text{cr})$  material equilibrated at  $T = 80\text{ }^\circ\text{C}$  in acidic NaCl solutions. This observation further confirms a solid phase transformation of  $\text{UO}_3 \cdot 2\text{H}_2\text{O}(\text{cr})$  into a sodium uranate like compound. However, after 290 days of equilibration it is not clear if this Na:U ratio reflects a final transformation stage or rather corresponds to a transient state and a further Na incorporation may be expected with longer equilibration times.

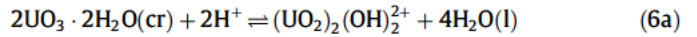
Results from the different analytical characterization techniques discussed above indicate that  $\text{Na}_2\text{U}_2\text{O}_7 \cdot \text{H}_2\text{O}(\text{cr})$  is a stable solid phase when equilibrated at  $T = 80\text{ }^\circ\text{C}$  in NaCl 0.51 mol/kg in the neutral to alkaline range, with temperature having a minor impact on the crystallinity. The same set of analyses further indicates that  $\text{UO}_3 \cdot 2\text{H}_2\text{O}(\text{cr})$  is unstable when equilibrated at  $T = 80\text{ }^\circ\text{C}$  in acidic NaCl solutions. The incorporation of  $\text{Na}^+$  cations into the layered structure of  $\text{UO}_3 \cdot 2\text{H}_2\text{O}(\text{cr})$  is a process known to occur even at room temperature, when the solid is contacted with  $\text{Na}^+$  containing solutions at neutral to alkaline  $\text{pH}_m$  conditions [17,37–39]. The formation of Na bearing U(VI) phases at room temperature and acidic conditions was previously reported by Diaz Arocas and Grambow [36]. Starting from oversaturation conditions, the authors observed the formation of  $\text{Na}_{0.33}\text{UO}_{3.165} \cdot 2\text{H}_2\text{O}(\text{cr})$  in 3 mol/kg NaCl solutions at  $\text{pH}_m = 4.6$ . The  $\log^*K'_{s,0}$  reported for this solid phase confirms its metastability with respect to the crystalline  $\text{UO}_3 \cdot 2\text{H}_2\text{O}(\text{cr})$  phase investigated in Altmaier et al. [20] and used as initial starting material in the present study. Although our results indicate a spontaneous transformation of  $\text{UO}_3 \cdot 2\text{H}_2\text{O}(\text{cr})$  into a sodium uranate like compound in acidic NaCl solutions at  $T = 80\text{ }^\circ\text{C}$ , conclusive evidence on the thermodynamic stability of this solid phase at room temperature is yet missing.

### 3.3. Chemical and thermodynamic models

The solubility of  $\text{UO}_3 \cdot 2\text{H}_2\text{O}(\text{cr})$  at  $\text{pH}_m = 4.5$  and  $T = 22\text{ }^\circ\text{C}$  is governed by the formation of  $\text{UO}_2^{2+}$  and  $(\text{UO}_2)_2(\text{OH})_2^{2+}$  according to reactions 5a and 6a. [20] The model is consistent with the observed trend of  $(\log[\text{U}] \text{ vs } \text{pH}_m)$ , characterized by a slope of 2 determined as in Eqs. (5b) and (6b) with the reasonable approximation made  $[\text{U}]_{\text{tot}} \approx [\text{UO}_2^{2+}] + [(\text{UO}_2)_2(\text{OH})_2^{2+}]$ .



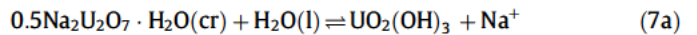
$$\log^* K'_{s,(1,0)} = \log[\text{UO}_2^{2+}] - 2 \log[\text{H}^+] \quad (5b)$$



$$\log^* K'_{s,(2,2)} = \log[(\text{UO}_2)_2(\text{OH})_2^{2+}] - 2 \log[\text{H}^+] \quad (6b)$$

At  $T = 80\text{ }^\circ\text{C}$ , a similar trend of  $\log[\text{U}] \text{ vs } \text{pH}_m$  is observed, hinting that the solubility of U(VI) may be controlled by analogous chemical reactions. Nonetheless, the partial transformation of  $\text{UO}_3 \cdot 2\text{H}_2\text{O}(\text{cr})$  into a sodium uranate like material described above prevents the development of reliable chemical and thermodynamic models for this system and boundary conditions.

The solubility of U(VI) in the neutral to moderately alkaline region ( $\text{pH}_m = 8-10$  at  $T = 22\text{ }^\circ\text{C}$ ,  $\text{pH}_m = 7.5-8$  at  $T = 80\text{ }^\circ\text{C}$ ) is mostly  $\text{pH}_m$  independent (see Fig. 1). Considering the only presence of  $\text{Na}_2\text{U}_2\text{O}_7 \cdot \text{H}_2\text{O}(\text{cr})$  in this  $\text{pH}_m$  region as discussed in Section 3.2, a chemical model based on the dissolution of  $\text{Na}_2\text{U}_2\text{O}_7 \cdot \text{H}_2\text{O}(\text{cr})$  and formation of  $\text{UO}_2(\text{OH})_3$  (1,3) can be defined (equation 7a). The corresponding conditional constants at  $T = 22$  and  $80\text{ }^\circ\text{C}$  ( $I = 0.51\text{ mol/kg NaCl}$ ) are calculated from the linear regression of the experimental  $\log[\text{U}] \text{ vs } \text{pH}_m$  data in these regions, according to Eq. (7b):

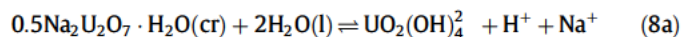


$$\log^* K'_{s,(1,3)} = \log[\text{UO}_2(\text{OH})_3] + \log[\text{Na}^+] \quad (7b)$$

with  $\log[\text{U}]_{\text{tot}} \approx \log[\text{UO}_2(\text{OH})_3]$ . The linear regression of both datasets results in  $\log^* K'_{s,(1,3)}$  (0.51 mol/kg NaCl,  $T = 22\text{ }^\circ\text{C}$ ) =  $(8.4 \pm 0.4)$  and  $\log^* K'_{s,(1,3)}$  (0.51 mol/kg NaCl,  $T = 80\text{ }^\circ\text{C}$ ) =  $(8.3 \pm 0.3)$ . Both solubility constants are very similar and reflect the minor impact of temperature on this equilibrium reaction. The value of  $\log^* K'_{s,(1,3)}$  (0.51 mol/kg NaCl,  $T = 22\text{ }^\circ\text{C}$ ) determined in this work is slightly lower than  $\log^* K'_{s,(1,3)}$  (0.51 mol/kg NaCl,  $T = 22\text{ }^\circ\text{C}$ ) =  $(8.1 \pm 0.5)$  reported previously for a non tempered  $\text{Na}_2\text{U}_2\text{O}_7 \cdot \text{H}_2\text{O}(\text{cr})$  phase [20], although both values agree within their large uncertainties.



In the alkaline region ( $\text{pH}_m > 11$  at  $T = 22^\circ\text{C}$ ,  $\text{pH}_m > 9$  at  $T = 80^\circ\text{C}$ ) the solubility is controlled by the formation of  $\text{UO}_2(\text{OH})_4^{2-}$  (1,4) according to reaction (8a). This is consistent with the slope of +1 in the trend of  $\log[U]$  vs  $\text{pH}_m$  observed for both temperatures (Eq. (8b); Fig. 1).



$$\log^* K'_{s,(1,4)} = \log[\text{UO}_2(\text{OH})_4^{2-}] + \log[\text{H}^+] + \log[\text{Na}^+] \quad (8b)$$

with  $\log[U]_{\text{tot}} \approx \log[\text{UO}_2(\text{OH})_4^{2-}]$ . Values of  $\log^* K'_{s,(1,4)}$  (0.51 mol/kg NaCl,  $T = 22^\circ\text{C}$ ) =  $(19.1 \pm 0.3)$  and  $\log^* K'_{s,(1,4)}$  (0.51 mol/kg NaCl,  $T = 80^\circ\text{C}$ ) =  $(16.9 \pm 0.1)$  are calculated according to equation 8b from the linear regression of the solubility data at  $T = 22$  and  $80^\circ\text{C}$ , respectively. Thus, the solubility of  $\text{Na}_2\text{U}_2\text{O}_7 \cdot \text{H}_2\text{O}(\text{cr})$  in the alkaline range at  $T = 80^\circ\text{C}$  is 2.2 orders of magnitude higher than the corresponding one at room temperature. An analysis of the calculated values of  $\log^* K'_{s,(1,4)}$  allows to ascribe this effect to three concurrent contributions occurring at the higher temperature: (i) increased acidity of water (in 0.51 mol/kg NaCl,  $\log K'_w = 13.84$  at  $T = 22^\circ\text{C}$ , and  $12.17$  at  $T = 80^\circ\text{C}$  [35]); (ii) enhanced stability of  $\text{UO}_2(\text{OH})_4^{2-}$  (endothermic effect); and (iii) decreased stability of  $\text{Na}_2\text{U}_2\text{O}_7 \cdot \text{H}_2\text{O}(\text{cr})$  reflecting an enhanced solubility strictly related to the solid phase and not to the hydrolysis species in solution. The contributions from (ii) and (iii) in the present work cannot be unambiguously separated; future calorimetric measurements of the dissolution enthalpy of  $\text{Na}_2\text{U}_2\text{O}_7 \cdot \text{H}_2\text{O}(\text{cr})$  are required to clearly separate both effects.

To properly compare the results in the alkaline range at the two temperatures, Fig. 4 shows the solubility of  $\text{Na}_2\text{U}_2\text{O}_7 \cdot \text{H}_2\text{O}(\text{cr})$  as a function of  $\log[\text{OH}^-]$ . This approach excludes the contribution of the temperature dependence of the water protolysis ( $\log K'_w(80^\circ\text{C}) = \log K'_w(22^\circ\text{C}) = 12.17 + 13.84 = +1.67$  log units) in the interpretation of the solubility data.

Fig. 4 shows that, when plotted as a function of  $\log[\text{OH}^-]$  instead of  $\text{pH}_m$ , the solubility of  $\text{Na}_2\text{U}_2\text{O}_7 \cdot \text{H}_2\text{O}(\text{cr})$  at  $T = 80^\circ\text{C}$

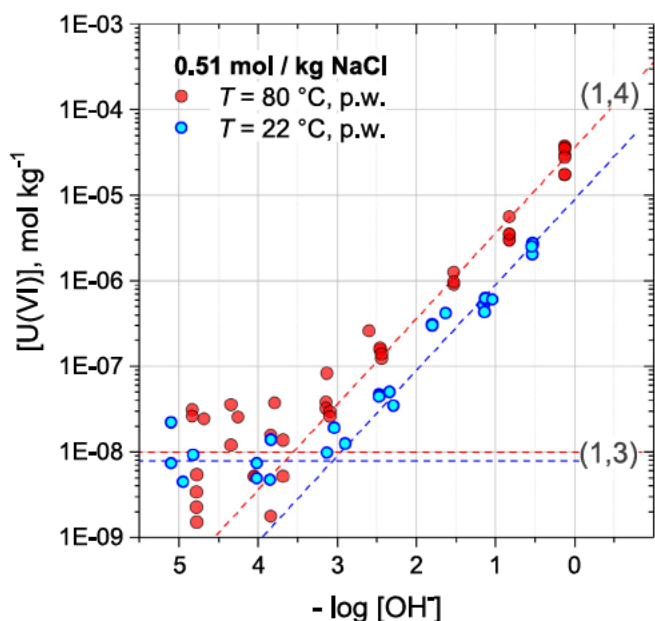


Fig. 4. Solubility of  $\text{Na}_2\text{U}_2\text{O}_7 \cdot \text{H}_2\text{O}(\text{cr})$  in 0.51 mol/kg of water NaCl solutions at  $T = 80^\circ\text{C}$  (red symbols) and  $T = 22^\circ\text{C}$  (blue symbols). Values of  $\text{pH}_m$  measured at  $T = 22$  and  $80^\circ\text{C}$  converted to  $[\text{OH}^-]$  as indicated in the text. (For interpretation of the references to colour in this figure legend, the reader is referred to the web version of this article.)

remains higher (+0.5 log units) than the one measured at  $T = 22^\circ\text{C}$ . This suggests that, although the solubility increase observed at  $T = 80^\circ\text{C}$  as a function of  $\text{pH}_m$  (see Fig. 1) can be largely attributed to the increased acidity of water, an endothermic contribution coming from the stabilization of  $\text{UO}_2(\text{OH})_4^{2-}$  at higher temperatures, as a result of a decreased stability of  $\text{Na}_2\text{U}_2\text{O}_7 \cdot \text{H}_2\text{O}(\text{cr})$ , or from the two latter effects must be also considered. Consistent with these observations, the formation of  $\text{UO}_2(\text{OH})_3$  through the pH independent reaction 7a is almost athermic.

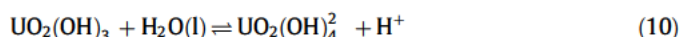
The enthalpies of reactions 7a and 8a in 0.51 mol/kg NaCl solutions were estimated from the calculated values of  $\log^* K'_{s,(1,3)}$  and  $\log^* K'_{s,(1,4)}$  at  $T = 22$  and  $80^\circ\text{C}$  using the Van't Hoff relation (9). This approach assumes  $d\Delta H/dT = 0$ , a reasonable approximation at  $T < 100^\circ\text{C}$  for most isoelectric processes like the one considered [45].

$$\Delta_r^* H_{m,(1,x)} \left( \frac{\text{kJ}}{\text{mol}} \right) = R \cdot (\ln 10) \cdot \frac{\log K'_{s,(1,x)}(T_1) - \log K'_{s,(1,x)}(T_2)}{1/T_2 - 1/T_1} \quad (9)$$

where  $R = 0.008314 \text{ kJ K}^{-1} \text{ mol}^{-1}$ ,  $T_1$  and  $T_2$  are the two temperatures in Kelvin (295 K, 353 K), and  $\log K'_{s,(1,x)}$  are the values of the conditional equilibrium constants for reactions 7a ( $x = 3$ ) and 8a ( $x = 4$ ) determined at  $T = 22$  and  $80^\circ\text{C}$  as previously explained. The calculated values are  $\Delta_r^* H_{m,(1,3)} = (4 \pm 14) \text{ kJ/mol}$  and  $\Delta_r^* H_{m,(1,4)} = (75 \pm 8) \text{ kJ/mol}$  for reactions 7a and 8a, respectively. The extrapolation of these values to  $I = 0$  using SIT [45–47] and neglecting the contribution of the term  $RT^2\Delta\epsilon_L$  (expectedly lower than 1 kJ/mol) resulted in  $\Delta_r H_{m,(1,3)}^0 = (3 \pm 14) \text{ kJ/mol}$  and  $\Delta_r H_{m,(1,4)}^0 = (72 \pm 8) \text{ kJ/mol}$ .

The values of  $\Delta_r^* H_{m,(1,3)}$ ,  $\Delta_r^* H_{m,(1,4)}$  calculated in the present work were derived from data collected at only two different temperatures. Such values and uncertainties should be therefore considered as best estimates, which reflect the limited dataset available and the inherent challenges of undertaking solubility experiments at elevated temperatures.

The dependence of the enthalpies on ionic strength is almost negligible and the enthalpy values at infinite dilution very close to those in 0.51 mol/kg NaCl. The values of  $\Delta_r H_{m,(1,3)}^0 = (3 \pm 14)$  and  $\Delta_r H_{m,(1,4)}^0$  can be combined to obtain the enthalpy of reaction (10):



with  $\Delta_r H_{m,(1,4)}^0 = \Delta_r H_{m,(1,3)}^0 + \Delta_r H_{m,(1,4)}^0 = (69 \pm 16) \text{ kJ/mol}$ . This value is slightly larger than the enthalpy associated to the hydrolysis of water ( $\text{H}_2\text{O}(\text{l}) \rightleftharpoons \text{H}^+ + \text{OH}^-$ , with  $\Delta_r H_{m,(1,3)}^0 = (55.8 \pm 0.1)$  at  $T = 25^\circ\text{C}$  [35], thus highlighting the stabilization of  $\text{UO}_2(\text{OH})_4^{2-}$  with respect to  $\text{UO}_2(\text{OH})_3$  with increasing temperature. Note that the value of  $\Delta_r H_{m,(1,4)}^0 = (69 \pm 16) \text{ kJ/mol}$  determined in the present work agrees well with  $\Delta_r H_{m,(1,4)}^0 = (73.9 \pm 2.5) \text{ kJ/mol}$  calculated in the present work from the enthalpies of formation of  $\text{UO}_2(\text{OH})_3$  and  $\text{UO}_2(\text{OH})_4^{2-}$  determined by Zanonato and co workers, based on a calorimetric study [5]. Provided the uncertainties discussed above with regard to the impact of  $\text{TMA}^+$  on the reported thermodynamic quantities, it is unclear whether the good agreement obtained for  $\Delta_r H_{m,(1,4)}^0$  is only a coincidence or rather reflects the expected insensitivity of enthalpy data to changes in the ionic medium [45–47].

The solubility constant of the  $\text{Na}_2\text{U}_2\text{O}_7 \cdot \text{H}_2\text{O}(\text{cr})$  phase pre-equilibrated at  $T = 80^\circ\text{C}$  was determined at  $T = 22^\circ\text{C}$  based upon the new experimental data ( $\log[U]$  vs.  $\text{pH}_m$ ) derived in this work.  $\log K'_{s,0}$  was calculated through a numerical optimization process. The quantity  $Q$  to be reduced (equation 11) was the sum of the squared residuals of the experimental  $\log[U]_{\text{exp}}$  and the corresponding values calculated from the mass balance equation ( $\log[U]_{\text{calc}}$ ).

**Table 2**  
Thermodynamic data determined in the present work and in Altmaier et al. [20] for solubility reactions involving  $\text{UO}_3 \cdot 2\text{H}_2\text{O}(\text{cr})$  and  $\text{Na}_2\text{U}_2\text{O}_7 \cdot \text{H}_2\text{O}(\text{cr})$ . Standard deviations are reported as  $2\sigma$ , accounting for 95% statistical confidence interval. Thermodynamic data reported in the NEA-TDB [9] and Altmaier et al. [20] for the same chemical reactions appended for comparison.

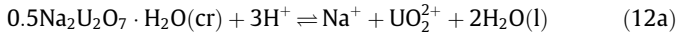
Chemical reaction	$\log^* K'_{s,0} \pm 2\sigma$	$T$ [°C]	Ref.
$\text{UO}_3 \cdot 2\text{H}_2\text{O}(\text{cr}) + 2\text{H}^+ \rightleftharpoons \text{UO}_2^{2+} + 3\text{H}_2\text{O}(\text{l})$	4.81 ± 0.43 (5.35 ± 0.13)	25 (22 ± 2)	[9] [20]
$0.5 \text{Na}_2\text{U}_2\text{O}_7 \cdot \text{H}_2\text{O}(\text{cr}) + 3\text{H}^+ \rightleftharpoons \text{Na}^+ + \text{UO}_2^{2+} + 2\text{H}_2\text{O}(\text{l})$	(12.2 ± 0.2) <sup>a</sup> <b>(11.9 ± 0.4)<sup>b</sup></b>	(22 ± 2) <b>(22 ± 3)</b>	[20] <b>p.w.</b>
	$\log^* K'_{s,(1,x)} \pm 2\sigma$	$\log^* K'_{s,(1,x)} \pm 2\sigma$	$\Delta_r H^{\circ}_{m,(1,x)} \pm 2\sigma$
		$I = 0.51 \text{ mol/kg NaCl}$	$\text{kJ/mol}$
$0.5 \text{Na}_2\text{U}_2\text{O}_7 \cdot \text{H}_2\text{O}(\text{cr}) + \text{H}_2\text{O}(\text{l}) \rightleftharpoons \text{Na}^+ + \text{UO}_2(\text{OH})_3$	-(8.5 ± 0.4) <b>-(8.9 ± 0.4)</b>	-(8.1 ± 0.5) <b>-(8.4 ± 0.4)</b>	(22 ± 2) <b>(22 ± 3)</b>
	<b>-(8.8 ± 0.3)</b>	<b>-(8.3 ± 0.3)</b>	<b>(80 ± 5)</b>
$0.5 \text{Na}_2\text{U}_2\text{O}_7 \cdot \text{H}_2\text{O}(\text{cr}) + 2\text{H}_2\text{O}(\text{l}) \rightleftharpoons \text{Na}^+ + \text{UO}_2(\text{OH})_4^{2-} + \text{H}^+$	-(19.7 ± 0.3) <b>-(20.1 ± 0.3)</b>	-(18.8 ± 0.4) <b>-(19.1 ± 0.3)</b>	(22 ± 2) <b>(22 ± 3)</b>
	<b>-(18.0 ± 0.1)</b>	<b>-(16.9 ± 0.1)</b>	<b>(72 ± 8)</b> <b>p.w.</b>

<sup>a</sup> Determined for a solid phase synthesized at  $T = 22$  °C.

<sup>b</sup> Determined for a solid phase synthesized at  $T = 22$  °C and equilibrated at  $T = 80$  °C for  $t = 290$  days.

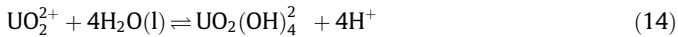
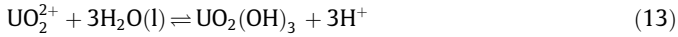
$$Q = \sum_i (\log [U]_{\text{exp}} - \log [U]_{\text{calc}})_i^2 \quad (11)$$

The speciation model used in the calculations included the definitions of  $\log^* K'_{s,0}$  (Eq. (12b)), together with values of  $\log^* \beta'_{(1,3)}$  and  $\log^* \beta'_{(1,4)}$  for reactions 13 and 14, respectively, as reported in Altmaier et al. [20].



$$\log^* K'_{s,0} = \log[\text{Na}^+] + \log[\text{UO}_2^{2+}] - 3 \log[\text{H}^+] \quad (12b)$$

and



Accordingly,  $\log^* K'_{s,0} = (12.3 \pm 0.4)$  was calculated ( $T = 22$  °C,  $I = 0.51$  mol/kg NaCl) for  $\text{Na}_2\text{U}_2\text{O}_7 \cdot \text{H}_2\text{O}(\text{cr})$ . The corresponding value at  $I = 0$  was obtained using the SIT ion interaction parameters summarized in Table S3 as Supporting Information, yielding  $\log^* K'_{s,0} = (11.9 \pm 0.4)$ . This value is slightly lower (0.3  $\log_{10}$  units) compared to the corresponding value previously determined with a non tempered  $\text{Na}_2\text{U}_2\text{O}_7 \cdot \text{H}_2\text{O}(\text{cr})$  phase [20]. This difference may be attributed to a modest increase of crystallinity of the solid phase as an effect of temperature. The corresponding value of  $\log^* K'_{s,0}$  for the system at  $T = 80$  °C cannot be calculated due to the lack of a reliable thermodynamic model including the temperature dependences of  $\log^* \beta'_{(1,3)}$  and  $\log^* \beta'_{(1,4)}$ .

Thermodynamic data determined in the present work and in Altmaier et al. [20] for solubility reactions involving  $\text{UO}_3 \cdot 2\text{H}_2\text{O}(\text{cr})$  and  $\text{Na}_2\text{U}_2\text{O}_7 \cdot \text{H}_2\text{O}(\text{cr})$  solid phases are summarized in Table 2. These data are used in thermodynamic calculations shown in Fig. 1 for the solubility of U(VI) at  $T = 22$  and  $80$  °C.

#### 4. Conclusions

The solubility of  $\text{UO}_3 \cdot 2\text{H}_2\text{O}(\text{cr})$  and  $\text{Na}_2\text{U}_2\text{O}_7 \cdot \text{H}_2\text{O}(\text{cr})$  in 0.51 mol/kg NaCl solutions was investigated at  $T = 22$  and  $80$  °C within the  $\text{pH}_m$  range 4–13.4 in order to assess the impact of elevated temperature on U(VI) solubility and hydrolysis. A comprehensive solid phase characterization was performed before and after the solubility experiments in order to analyze structural changes in solid phase due to the equilibration of samples at elevated temperature.

In the acidic  $\text{pH}_m$  range, the solubility of  $\text{UO}_3 \cdot 2\text{H}_2\text{O}(\text{cr})$  at  $T = 80$  °C is approximately one order of magnitude lower than at  $T = 22$  °C.

Solid phase characterization by XRD, SEM EDS and quantitative chemical analyses evidences the transformation of  $\text{UO}_3 \cdot 2\text{H}_2\text{O}(\text{cr})$  into a sodium uranate like phase after equilibrating the initial solid material at  $T = 80$  °C in 0.51 mol/kg NaCl solution at  $\text{pH}_m = 4.5$ . Long term solubility experiments are on going to analyze the long term stability of this alteration phase.

Solubility data and solid phase characterizations confirm that  $\text{Na}_2\text{U}_2\text{O}_7 \cdot \text{H}_2\text{O}(\text{cr})$  is the thermodynamically stable solid phase in 0.51 mol/kg NaCl solutions in near neutral to alkaline  $\text{pH}_m$  conditions, both at room temperature and at  $T = 80$  °C. The solubility of  $\text{Na}_2\text{U}_2\text{O}_7 \cdot \text{H}_2\text{O}(\text{cr})$  at  $\text{pH} > 7$  is governed by the equilibria with  $\text{UO}_2(\text{OH})_3$  and  $\text{UO}_2(\text{OH})_4^{2-}$  hydrolysis species, forming at  $[\text{OH}^-]$  below and above  $\approx 10^{-3}$  m, respectively. Solubility data indicate that the equilibrium reaction  $0.5 \text{Na}_2\text{U}_2\text{O}_7 \cdot \text{H}_2\text{O}(\text{cr}) + \text{H}_2\text{O}(\text{l}) \rightleftharpoons \text{UO}_2(\text{OH})_3 + \text{Na}^+$  is not significantly affected by temperature. In contrast to this finding, the conditional stability constant for the equilibrium reaction relevant for higher alkaline  $\text{pH}_m$  conditions,  $0.5 \text{Na}_2\text{U}_2\text{O}_7 \cdot \text{H}_2\text{O}(\text{cr}) + 2 \text{H}_2\text{O}(\text{l}) \rightleftharpoons \text{UO}_2(\text{OH})_4^{2-} + \text{H}^+ + \text{Na}^+$ , is increased  $>2$  orders of magnitude at  $T = 80$  °C compared to room temperature conditions. This is primarily due to the enhanced acidity of water at elevated temperatures. An additional endothermic contribution resulting from the stabilization of  $\text{UO}_2(\text{OH})_4^{2-}$  or a decreased stability of  $\text{Na}_2\text{U}_2\text{O}_7 \cdot \text{H}_2\text{O}(\text{cr})$  is further required to explain the experimental data collected at  $T = 80$  °C. Based on the new solubility data presented in this work, a thermodynamic model was derived including the values of the conditional constants (0.51 mol/kg NaCl) for the solubility equilibria of  $\text{Na}_2\text{U}_2\text{O}_7 \cdot \text{H}_2\text{O}(\text{cr})$  leading to the formation of  $\text{UO}_2(\text{OH})_3$  and  $\text{UO}_2(\text{OH})_4^{2-}$  ( $\log^* K'_{s,(1,3)} = (8.4 \pm 0.4)$ ,  $(8.3 \pm 0.3)$ ,  $\log^* K'_{s,(1,4)} = (19.1 \pm 0.3)$ ,  $(16.9 \pm 0.1)$  at  $T = 22$  and  $80$  °C, respectively). From the temperature dependence of these constants, the corresponding enthalpy values were calculated. These thermodynamic quantities can be used for modelling the solubility behavior of U(VI) in alkaline NaCl solutions within the temperature range 22–80 °C.

To the best of our knowledge, this work presents the first quantitative analysis of the impact of temperature on the solubility of U(VI) under alkaline to hyperalkaline  $\text{pH}_m$  conditions. The successful experimental and conceptual approach used in this study opens new perspectives on the study of U(VI) hydrolysis in the alkaline  $\text{pH}_m$  range, where the low solubility of M-uranate phases (with  $M = \text{Na, K, Li, Ca, \dots}$ ) poses limitations to the use of other established methods such as potentiometry or spectroscopy. This approach requires exhaustive solid phase characterization before and after the solubility experiments in order to identify possible temperature induced alterations of the solubility controlling solid phases.



## Acknowledgment

The authors would like to thank F. Geyer, C. Walschburger, M. Böttle, S. Heck, S. Moisei Rabung, T. Kisely and E. Soballa (KIT INE) for their lab assistance and ICP MS, ICP OES, TG DTA, TOC and SEM EDS analyses.

This work was partially funded by the German Federal Ministry for Education and Research (BMBF). KIT INE is working in Ther mAc under the contract O2NUK039A.

## Appendix A. Supplementary data

Supplementary data associated with this article can be found, in the online version, at <https://doi.org/10.1016/j.jct.2018.01.006>.

## References

- [1] Project Opalinus Clay. Safety Report: Demonstration of disposal feasibility for spent fuel, vitrified high-level waste and long-lived intermediate-level waste (Entsorgungsnachweis); 2002.
- [2] V. Metz, H. Geckeis, E. Gonzalez-Robles, A. Loida, C. Bube, B. Kienzler, *Radiochim. Acta* 100 (8–9) (2012) 699–713.
- [3] L. Rao, T.G. Srinivasan, A.Y. Garnov, P. Zanonato, B. Di Plinio, A. Bismondo, *Geochim. Cosmochim. Acta* 68 (23) (2004) 4821–4830.
- [4] P.L. Zanonato, P. Di Bernardo, A. Bismondo, G. Liu, X. Chen, L. Rao, *J. Am. Chem. Soc.* 126 (17) (2004) 5515–5522.
- [5] P.L. Zanonato, P. Di Bernardo, I. Grenthe, *Dalt. Trans.* 43 (6) (2014) 2378–2383.
- [6] J. Hála, H. Miyamoto, *J. Phys. Chem. Ref. Data* 36 (4) (2007) 1417–1736.
- [7] D.J. Wronkiewicz, E.C. Buck (Uranium) *Rev. Mineral.* 38 (1999) 475–497.
- [8] M.E. Torrero, I. Casas, J. de Pablo, M.C.A. Sandino, B. Grambow, *Radiochim. Acta* 66 (67) (1994) 29–35.
- [9] R. Guillaumont T. Fanghänel V. Neck J. Fuger D.A. Palmer I. Grenthe M. Rand Update on the Chemical Thermodynamics of Uranium, Neptunium, Plutonium, Americium and Technetium, OECD Nuclear Energy Agency, Thermodynamic Data Bank: Issy-les-Moulineaux, France, 2003.
- [10] T.E. Eriksen, D.W. Shoosmith, M. Jonsson, *J. Nucl. Mater.* 420 (1–3) (2012) 409–423.
- [11] R.J. Finch, M.A. Cooper, F.C. Hawthorne, R.C. Ewing, *Can. Mineral.* 34 (5) (1996) 1071–1088.
- [12] R.J. Finch, F.C. Hawthorne, *Can. Mineral.* 36 (3) (1998) 831–845.
- [13] A.G. Sowder, S.B. Clark, R.A. Fjeld, *Environ. Sci. Technol.* 33 (20) (1999) 3552–3557.
- [14] D. Gorman-Lewis, P.C. Burns, J.B. Fein, *J. Chem. Thermodyn.* 40 (3) (2008) 335–352.
- [15] R.J. Finch, E.C. Buck, P.A. Finn, J.K. Bates (Scientific Basis for Nuclear Waste Management XXII) *Mater. Res. Soc. Symp. Proc.* 556 (1999) 431–438.
- [16] P.C. Burns, *Canad. Mineral.* 43 (2005) 1839–1894.
- [17] D.E. Giammar, J.G. Hering, *Environ. Sci. Technol.* 38 (1) (2004) 171–179.
- [18] D.E. Giammar, *Geochemistry of uranium at mineral-water interfaces: rates of sorption-desorption and dissolution-precipitation reactions*, California Institute of Technology, 2001.
- [19] V. Baran, M. Tympl, *Zeitschrift fuer Anorg. und Allg. Chemie* 347 (3–4) (1966) 184–190.
- [20] M. Altmaier, E. Yalcintas, X. Gaona, V. Neck, R. Mueller, M. Schlieker, T. Fanghaenel, *J. Chem. Thermodyn.* (2017), accepted.
- [21] I. Grenthe J. Fuger R.J.M. Konings R.J. Lemire A.B. Muller C. Nguyen-Trung H. Wanner Chemical Thermodynamics of Uranium H. Wanner I. Forest OECD Nuclear Energy Agency, Thermodynamic Data Bank Issy-les-Moulineaux (France), 1992.
- [22] P.L. Brown, C. Ekberg, *Hydrolysis of Metal Ions*, Wiley-VCH, Verlag GmbH & Co KGaA, Weinheim, 2016.
- [23] M. Altmaier, X. Gaona, T. Fanghaenel (Washington, DC, United States) *Chem. Rev.* 113 (2) (2013) 901–943.
- [24] E.I. Sergeeva, A.A. Nikitin, I.L. Khodakovskii, G.B. Naumov, *Geokhimiya* (11) (1972) 1340–1350.
- [25] N.M. Nikolaeva, A.V. Pirozhkov, *Izv. Sib. Otd. Akad. Nauk SSSR, Seriya Khimicheskikh Nauk* (4) (1971) 73–81.
- [26] R.J. Lemire, P.R. Tremaine, *J. Chem. Eng. Data* 25 (4) (1980) 361–370.
- [27] E. Valsami-Jones, K.V. Ragnarsdottir, *Radiochim. Acta* 79 (4) (1997) 249–257.
- [28] C.F. Baes Jr., N. Meyer, *J. Inorg. Chem.* 1 (1962) 780–789.
- [29] N.M. Nikolaeva, *Izv. Sib. Otd. Akad. Nauk SSSR, Seriya Khimicheskikh Nauk* (3) (1971) 61–67.
- [30] A.A. Nikitin, E.I. Sergeeva, I.L. Khodakovskii, G.B. Naumov, *Geokhimiya* (3) (1972) 297–307.
- [31] P.L. Zanonato, Z. Szabo, V. Vallet, P. Di Bernardo, I. Grenthe, *Dalt. Trans.* 44 (37) (2015) 16565–16572.
- [32] P.L. Zanonato, P. Di Bernardo, I. Grenthe, *Dalt. Trans.* 41 (12) (2012) 3380–3386.
- [33] J.D. Cox, D.D. Wagman, V.A. Medvedev, *CODATA Key Values for Thermodynamics*, Hemisphere Publ. Corp., 1989.
- [34] I.R. Tasker, P.A.G. O'Hare, B.M. Lewis, G.K. Johnson, E.H.P. Cordfunke, *Can. J. Chem.* 66 (4) (1988) 620–625.
- [35] J.D. Cox, D.D. Wagman, V.A. Medvedev, *CODATA Key Values for Thermodynamics*, Hemisphere Publ. Corp., 1989.
- [36] P.D. Arocas, B. Grambow, *Geochim. Cosmochim. Acta* 62 (2) (1998) 245–263.
- [37] T. Fanghanel, V. Neck, *Pure Appl. Chem.* 74 (10) (2002) 1895–1907.
- [38] D.E. Giammar, J.G. Hering, *Geochim. Cosmochim. Acta* 66 (18) (2002) 3235–3245.
- [39] D. Gorman-Lewis, J.B. Fein, P.C. Burns, J.E.S. Szymanowski, J. Converse, *J. Chem. Thermodyn.* 40 (6) (2008) 980–990.
- [40] G.H. Jeffrey, J. Bassett, J. Mendham, R.C. Denney, *Vogel's Textbook of Quantitative Chemical Analysis*, 5th., John Wiley & Sons, 1990.
- [41] L. Ciavatta, *Ann. Chim.* 70 (1980) 551.
- [42] P.C. Debets, B.O. Loopstra, *J. Inorg. Nucl. Chem.* 25 (8) (1963) 945–953.
- [43] R.J. Finch, R.C. Ewing, *Am. Mineral.* 82 (5–6) (1997) 607–619.
- [44] L.M. Kuznetsov, A.N. Tsvigunov, *Radiokhimiya* 18 (3) (1976) 414–416.
- [45] I. Grenthe I. Puigdomènech B. Allard *Modelling in Aquatic Chemistry*; Nuclear Energy Agency, Organisation for Economic Co-operation and Development, 1997
- [46] A.V. Plyasunov, I. Grenthe, *Geochim. Cosmochim. Acta* 58 (17) (1994) 3561–3582.
- [47] I. Puigdomènech J.A. Rard A.V. Plyasunov I. Grenthe. Temperature corrections to thermodynamic data and enthalpy calculations; *Le Seine-St. Germain* 12, Bd. des Îles F-92130 Issy-les-Moulineaux FRANCE, 1999.